PAPER NO: TP09-12
CATEGORY: TESTING

COOLING TECHNOLOGY INSTITUTE

A REYNOLDS NUMBER CORRECTION FOR PITOT MEASUREMENTS

DUDLEY BENTON
MCHALE & ASSOCIATES

Presented at the 2009 Cooling Technology Institute Annual Conference
San Antonio, TX - February 8-12, 2009

A Reynolds Number Correction for Pitot Measurements

Dudley J. Benton, Ph.D., Principal Engineer
McHale & Associates, Inc., Knoxville, TN
(865)588-2654x116 dudley.benton@mchale.org

Abstract

The Pitot tube has been the mainstay of flow measurement in cooling towers for decades, but this is not the only application for velocity probes of this type. Unlike the cooling tower flow measurement techniques prescribed by the CTI, most other applications of these and similar probes consider the Reynolds Number, typically at the head of the probe. The correction for Reynolds Number in the derived correlations for such probes is iterative, but easily implemented and converges quickly. The information necessary to incorporate a correction for Reynolds Number is often collected (but not used) along with the other data when the probe is being calibrated. This paper will explore the efficacy of utilizing a local Reynolds Number correction with several Pitot probes and whether or not this actually reduces the overall uncertainty of the final flow measurement.

Introduction

Accurate measurement of water flow is an essential part of determining the performance of any heat exchanger, especially a cooling tower (Section 5.1, CTI 1995 and Section 3.1, CTI, 2000). In fact, the most common parameter used to express cooling tower performance, capability, is directly proportional to water flow (Section 6.3, CTI 2000). While there are several methods available for measuring water flow, from propeller meters to Doppler anemometry, the most commonly accepted and used method is a Pitot probe traverse of a round pipe, and occasionally of a rectangular duct using the same instrument. Much effort has been invested in calibrating these devices under laboratory conditions as close to field conditions as possible and identifying the limitations of these devices to stay within prescribed bounds or add caveats when this is not practical (Section 3.4, CTI 1995).

Flow Constant of Proportionality

In spite of the fact that a traverse is almost always performed, over which multiple local differential pressure measurements are taken, implicitly recognizing the existence of a variable velocity profile, this calibration process has primarily been focused on determining a bulk or average multiplying factor from which to infer total flow. Averaging these multiple local differential pressure measurements, whether weighted for fractional areas or not, and correlating the results to values of flow, is an integration process based on the definition of flow, Equation 1:

$$Q = \int_0^{2\pi}\int_0^{R} V\, r\, dr\, d\theta \qquad \textbf{(1)}$$

The integration with respect to circumferential angle, θ, has not been simplified in Equation 1; because two traverses are often made, 90° apart, in order to capture asymmetrical effects. The drag (or pressure) coefficient is a constant of proportionality that relates the pressure drop and velocity as in Equation 2.

$$\Delta p = C_D \frac{\rho V^2}{2 g_c} \qquad \textbf{(2)}$$

This relationship (Equation 2) can be substituted into Equation 1 in order to obtain an expression for the flow as a function of the pressure drop and pressure coefficient, Equation 3:

$$Q = \int_0^{2\pi}\int_0^{R} \sqrt{\frac{2g_c \Delta p}{\rho C_D}}\, r\, dr\, d\theta \qquad \textbf{(3)}$$

This relationship (Equation 3) is traditionally simplified by defining an effective average constant of proportionality, C_A, as in Equation 4:

$$\frac{\int_0^{2\pi}\int_0^{R} \Delta p\, r\, dr\, d\theta}{\pi R^2} = C_A \frac{\rho_A V_A^2}{2g_C} \qquad \textbf{(4)}$$

Where V_A is the average velocity and ρ_A is the average density. These are related to the flow by Equation 5:

$$Q = \pi R^2 V_A \qquad \textbf{(5)}$$

Substituting Equation 5 into Equation 4 and solving for C_A yields Equation 6.

$$C_A = \left(\frac{\pi R^2 g_C}{\rho_A Q^2}\right) \int_0^{2\pi}\int_0^{R} \Delta p\, r\, dr\, d\theta \qquad \textbf{(6)}$$

Substituting Equation 2 into Equation 6 and assuming constant density yields Equation 7, relating the local and average constants of proportionality:

$$C_A = \int_0^{2\pi}\int_0^{R} C_D \left(\frac{V}{V_A}\right)^2 \left(\frac{\rho}{\rho_A}\right) \frac{r}{R}\, \frac{dr}{R}\, \frac{d\theta}{\pi} \qquad \textbf{(7)}$$

Pressure Coefficients

The end of a Pitot probe is always some shape whose flow characteristics have been extensively studied, such as a cylinder, prism, or wing. The pressure coefficient for common shapes can be found in any text on fluid mechanics, typically in a graph showing the variation with Reynolds Number as in Figure 1, which is a composite of several such graphs.

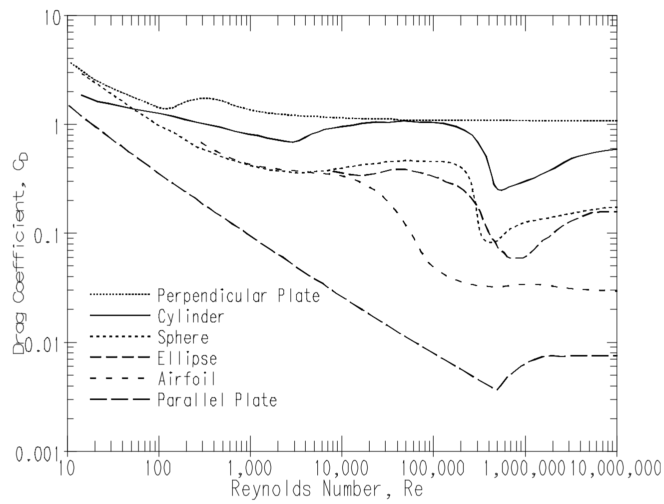

Figure 1. Drag Coefficient for Various Shapes

Not only does the pressure differential, Δp, vary with radius and circumferential angle, but also the coefficient, C_D, varies. The local velocity always varies from some maximum to zero over the radius; and the Reynolds Number is proportional to the velocity; therefore, the pressure coefficient can be expected to vary in a manner similar to the curves shown in Figure 1. Over some part of these curves the variation is either negligible or linear; however, for Reynolds Numbers between 3000 and 500,000 the curves exhibit significant variability. Use of an effective average constant of proportionality when some significant part of the flow is in this range without correcting for Reynolds Number is likely to be problematic and may result in greater calibration uncertainty.

The first dip in the cylinder curve in Figure 1 bottoms-out at a Reynolds Number of 2885. For an 0.625 inch (1.6 cm) diameter probe in water this corresponds to 0.67 ft/s (0.20 m/s). For the same probe in air this corresponds to 8.7 ft/s (2.7 m/s). The most common applications for such probes in water range in velocity from 0 to 11 ft/s (3.3 m/s) and in air from 0 to 33 ft/s (10 m/s), putting them in this transitional region of the significant Reynolds Number dependence of proportionality nstant. This observation is the impetus for the analysis presented here.

Cylindrical Probes

The measured pressure coefficient for a right, circular cylinder in a crossflow, as shown in Figure 1, can be used along with typical velocity profiles in order to investigate the magnitude of the impact on the calculation of flow. For flow in a pipe with a circular cross-section the only unknowns become the Reynolds Number at the bulk velocity and the ratio of the pipe to probe diameters, β=d/D. Typical turbulent velocity profiles in a cylindrical pipe are shown in Figure 2. The Reynolds Number shown in Figure 2 is for the bulk flow and is based on the pipe diameter.

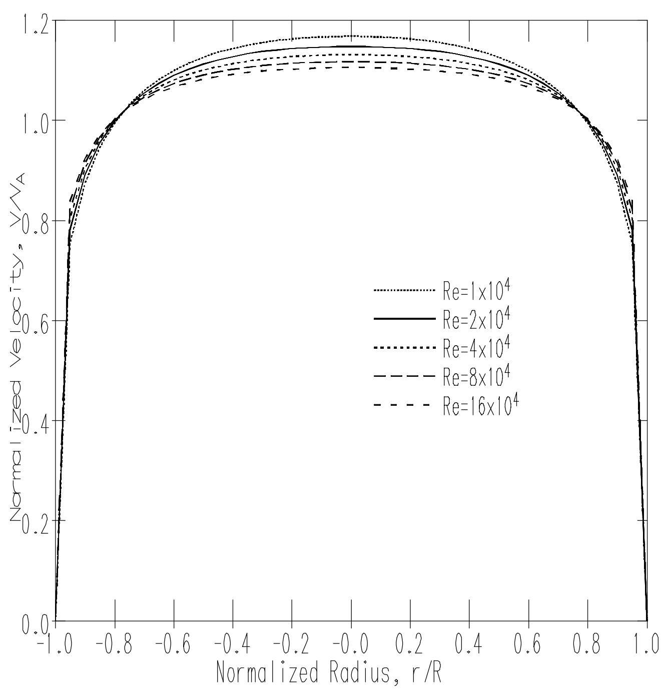

Figure 2. Normalized Velocity Profiles

Use of a power-law velocity profile dates back to the early work of von Karman in 1930 (as cited by Zanoun, Durst, and Nagib 2003, who provide updated coefficients). A very important historical publication on this subject is that of Johnson and Bushnell 1970, which discusses the variation with Reynolds Number in detail. Some additional considerations for pipe flow are provided by Rudman, Blackburn, Graham, and Pullum 2001.

The area under the curves in Figure 2 are not equal; because the assumed velocity profiles are three-dimensional and axisymmetric. The volumes are equal when integrated with the radius, as in Equation 1. This being the case, it is interesting to note that the slight bulging of the profiles on the sides (near r/R=±0.8), while it may seem to occupy a much smaller area in this two-dimensional profile view, is of equal significance to the bulging at the top (r/R<0.5). The integral (Equation 1) contains the terms r dr; therefore, the contribution to the whole of each point along the velocity profile is proportional to the radius at that point. This means that variations toward the walls (r/R>0.5) have a greater contribution than those closer to the centerline (r/R<0.5).

The cylinder pressure coefficient, C_D, from Figure 1 can be computed at the local Reynolds Number based on the local velocity curves from Figure 2 and the probe diameter. Figure 3 shows the variation in $1/C_D$ for a pipe to probe diameter ratio of 24 (for instance, a 0.625 inch (1.6 cm) diameter probe in a 15 inch (0.38 m) diameter pipe). The inverse is plotted vs. radius; because as r approaches R at the wall, the velocity goes to zero, as does the Reynolds Number. As shown in Figure 2 (which has log-log scales) C_D approaches infinity as Reynolds Number approaches zero.

The range of bulk Reynolds Number shown in Figures 2 and 3 is consistent with typical applications where a Pitot probe might be used. Notice that the $1/C_D$ profiles in Figure 3 have significantly different shapes. These variations in shape reveal that the local probe Reynolds Number crosses the region shown in Figure 1 where C_D is highly nonlinear. As with the velocity, when computing an integrated average pressure coefficient for a probe, the contribution to the whole is proportional to the radius, so that the variations toward the walls have a greater

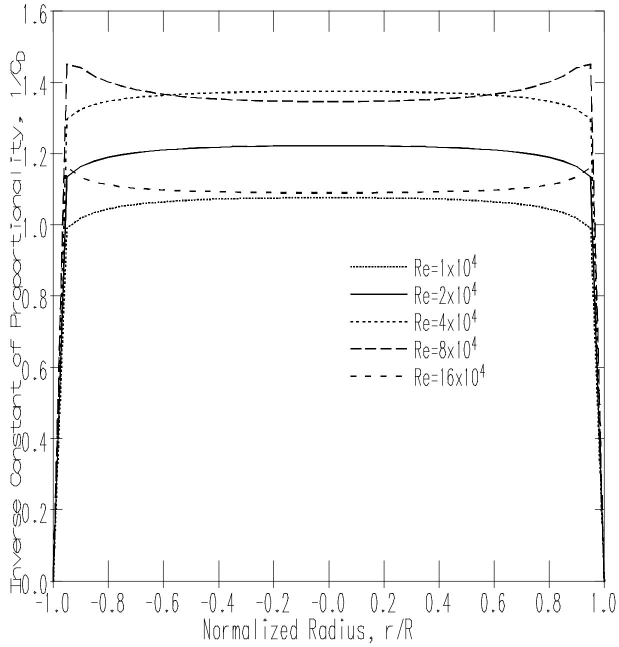

Figure 3. Inverse Constant of Proportionality

influence on than those closer to the centerline. Specifically, in Figure 3, the flat portion of the profiles does not account for as much of the total flow area as the curved portion of the profiles; and the shape of the curved portion of the profiles changes with bulk Reynolds Number.

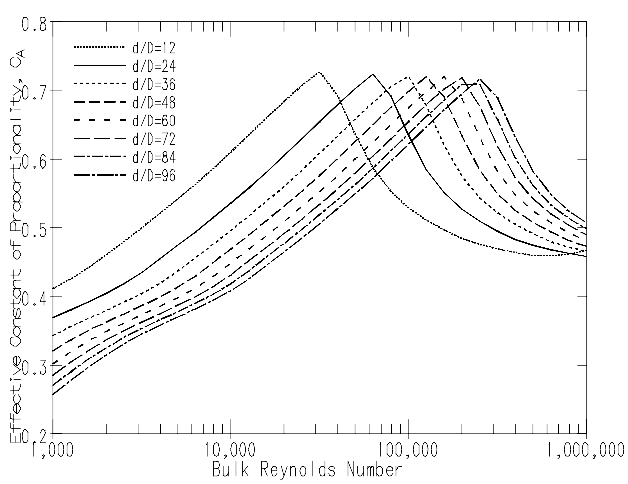

Figure 4. Effective Coefficient for a Cylinder

The effective average pressure coefficient can be found by combining Equations 6, Figure 1 and Figure 2. This is plotted over a range of Reynolds Numbers and for various values of the probe to pipe diameter ratio, β, in Figure 4.

Figure 4 would seem to indicate that the calibration coefficient for a Pitot probe (i.e., it's effective average coefficient of proportionality) can be expected to vary not only with bulk Reynolds Number, but also with the diameter of pipe in which it is used--and this is for an ideal axisymmetric velocity distribution. Experience bears this out, which is why so much effort is devoted to calibrating Pitot probes in large test facilities and why caveats are added when the probe is used outside the calibration parameters.

Laboratory Calibration Data

It is not the intention of this analysis to replace laboratory calibration of Pitot probes, only to better understand and possibly improve calibration. One practical benefit of this analysis would be if it can be used somehow to expand the range of conditions in which a probe could be used with comparable uncertainty or even reduce the uncertainty. Actual laboratory calibration data are used to evaluate this possibility. Perhaps the most commonly used probe is the Simplex, which is shown in Figure 5. A search of the U. S. Patent Office records indicates that the first mention of this device was by the Geo. H. Gibson Company in 1918 (Gibson 1918 in Amir and Peranio 1972). The devices were manufactured by the Simplex Valve & Meter Co. and later by Leupold & Stevens, Inc. of Beaverton, OR.

Laboratory calibration data are considered for 80 cases involving 14 different Simplex probes. Each consists of 20 differential pressure measurements traversing the diameter of a round pipe plus the total flow. Two traverses at 90° are available for 74 of the 80 cases. Taking two traverses at 90° is a common practice, especially in the field; because the velocity profile is probably not symmetric. A typical pair of velocity profiles for the two traverses is shown in Figure 6 along with the ideal power-law profile.

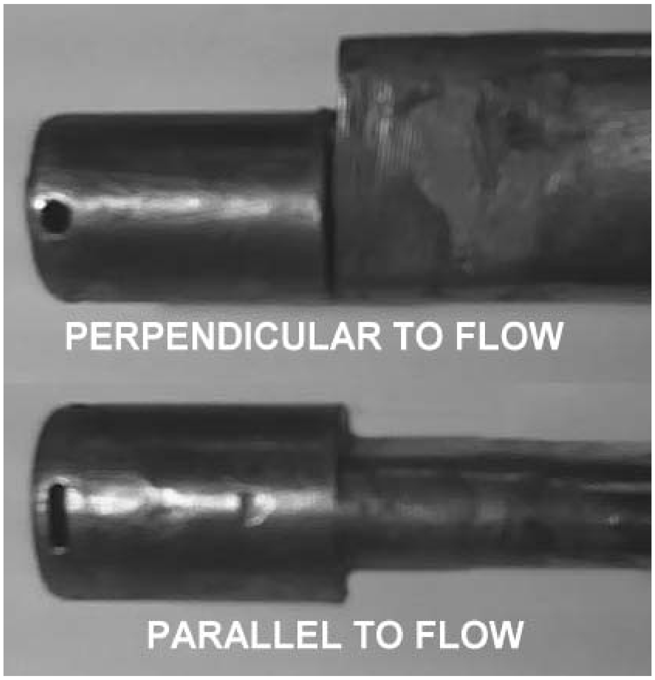

Figure 5. The Simplex Probe

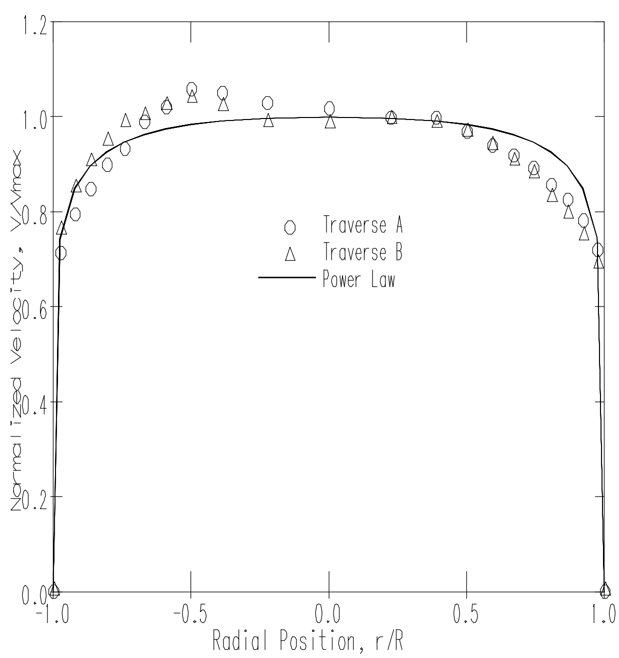

Figure 6. Typical Laboratory Velocity Profiles

As shown in Figure 6, in spite of the fact that these measurements were taken in a laboratory under carefully controlled conditions in a test section having a very long straight run of pipe upstream, the velocity profiles deviate noticeably from the ideal symmetry. It can also be seen in this figure that the power-law profile does fit the data fairly well. These two are typical of the 154 profiles considered.

Equation 7 with C_D=1 is traditionally used to determine the "Pitot Calibration Coefficient" or constant of proportionality for a given probe. For the 80 cases consisting of 154 profiles for 14 Simplex probes, the mean value of C_A was determined to be 0.793 with a 95% confidence interval of ±0.029, a minimum of 0.766, and a maximum of 0.820. If, however, Equation 7 is used with a variable C_D based on the local Reynolds Number and the pressure coefficient for a cylinder as shown in Figure 1, this "Corrected Pitot Calibration Coefficient" was found to have a mean of 0.818 with a 95% confidence interval of ±0.026, a minimum of 0.791, and a maximum of 0.845. This method of incorporating the impact of Reynolds Number results in a decrease in the ratio of uncertainty to mean of 19%; so there is some advantage to correcting Simplex probe data in this way. The coefficients are shown in Figure 7 along with the corresponding 95% confidence interval:

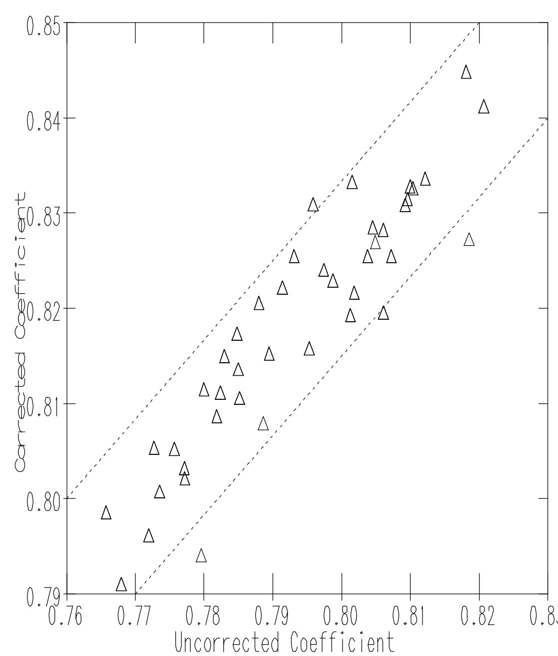

Figure 7. Laboratory Pitot Coefficients

Alternate Probe Shapes

As indicated before, the typical range of operation for Simplex probes spans the portion of the pressure coefficient for a cylinder which exhibits pronounced changes. The pronounced changes were shown in Figure 1 and the result of using the pressure coefficient in Equation 7 was shown in Figure 4. Some validity to this calculation was shown by a reduction in the variability of laboratory calibration coefficients. With these considerations in mind, it seems reasonable to use the pressure coefficient for other shapes in these same calculations in order to get some indication as to the relative appropriateness of these shapes for use as a probe design. An ideal shape for a probe would be one that has a constant pressure coefficient, independent of Reynolds Number, or a flat line on Figure 1. A set of curves like Figure 4 can be created for each of the shapes in Figure 1.

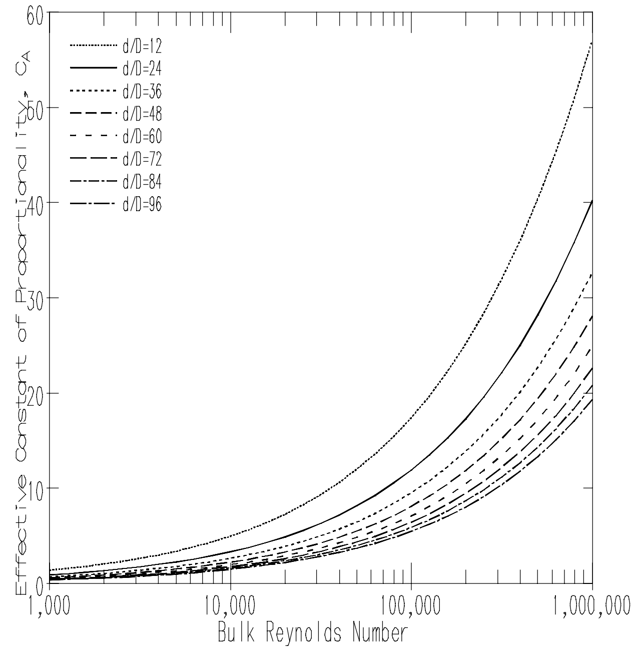

Figure 9. Effective Coefficient for a Plate

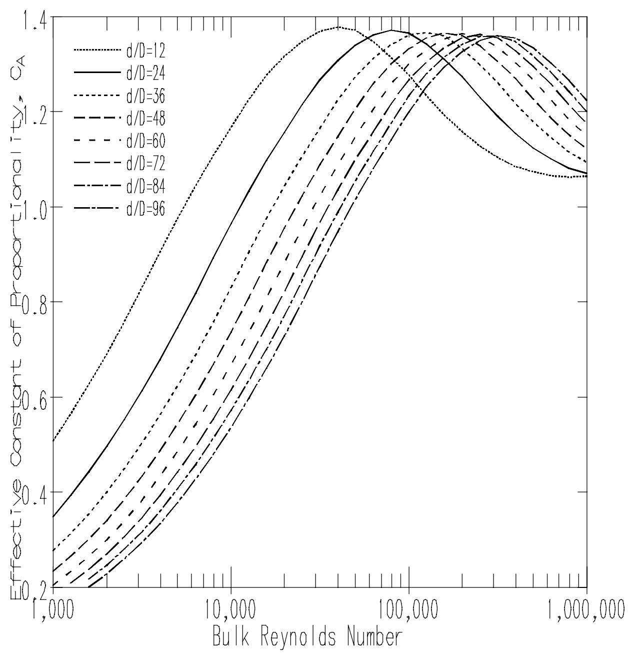

Figure 8. Effective Coefficient for a Sphere

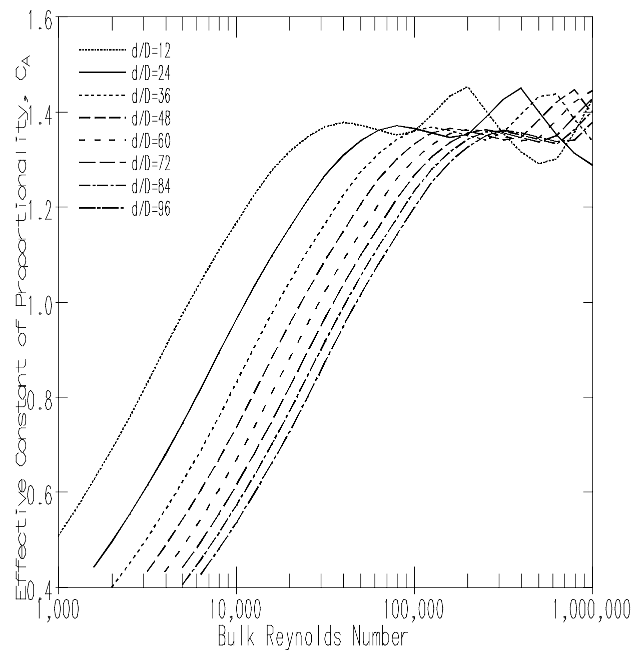

Figure 10. Effective Coefficient for an Ellipse

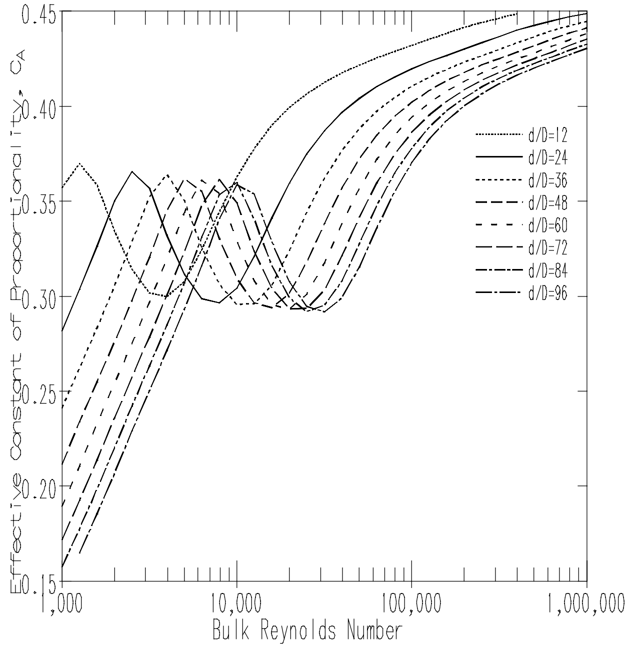

Figure 11. Effective Coefficient for a Disk

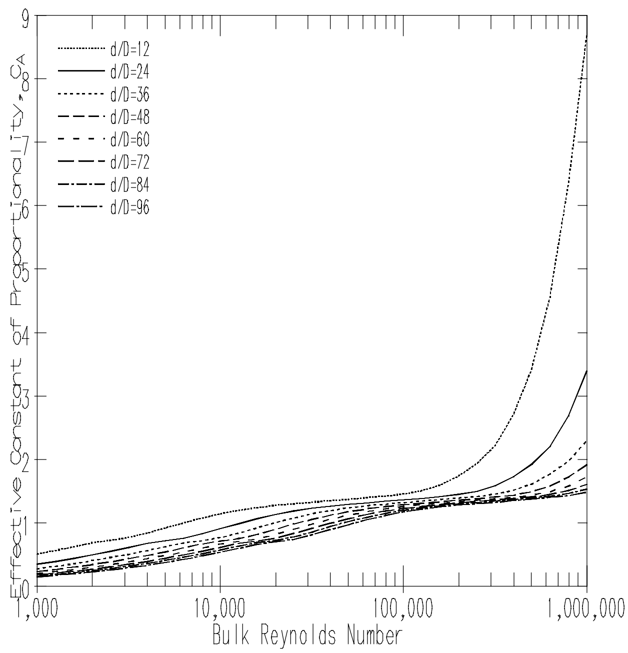

Figure 12. Effective Coefficient for an Airfoil

Figures 4 and 8 through 12 show that those shapes having the most complexly varying pressure coefficients (cylinder, sphere, and ellipse) or the most variable in magnitude (plate) would result in the most variable effective average coefficient of proportionality, making these the least attractive choices. The one having the least variable pressure coefficient (disk) produces the least variable effective average coefficient of proportionality, making it the most attractive choice. The airfoil shape might also be an attractive choice, provided the bulk Reynolds Number is not too large and the probe to pipe diameter is not too small.

Summary

In summary, the impact of Reynolds Number and probe to pipe diameter ratio has been discussed for Pitot probes, with particular focus on the Simplex design. The Simplex design has been analyzed as a cylinder in a crossflow. Laboratory calibration data have been presented and a Reynolds Number correction for the cylindrical shape applied. This correction reduced the ratio of 95% confidence interval to mean value of the constant of proportionality by 19%, indicating some advantage to this analysis. Effective average coefficients of proportionality were computed for a cylinder, sphere, ellipse, plate, disk, and airfoil, based on the respective pressure coefficients. Comparison of the effective average coefficients of proportionality indicate that the cylinder, sphere, ellipse, and plate shapes would not be attractive choices for a probe; whereas, the disk and airfoil would be attractive choices.

Conclusions

The Simplex probe, being cylindrical in shape, can be expected to exhibit a calibration dependence on Reynolds Number and probe to pipe diameter ratio. This dependence can be accounted for to some extent by utilizing the pressure coefficient for a cylinder in a crossflow. The confidence interval in the coefficient of proportionality for the Simplex probe can be reduced by incorporating the dependence of the pressure coefficient with Reynolds Number in the calibration data. A different probe shape, possibly a disk or ellipse, should be more attractive than the cylinder.

Recommendations

This same analysis should be applied to laboratory calibration data for probes other than the Simplex and a comparison made. Several different shaped probes should be fabricated and tested. As roughness has been shown in some cases to stabilize the onset of turbulence and separation, artificially roughened probes should also be tested.

Symbols

C_D . . . . pressure coefficient [unitless]
d . . . . probe diameter [l]
D . . . . pipe diameter [l]
g . . . . acceleration of gravity [l/t^2]
g_c . . . . mass conversion factor [ml/Ft^2]
p . . . . pressure [F/l^2]
Q . . . . flow [l^3/t]
r . . . . distance from centerline [l]
R . . . . radius [l]
V . . . . velocity [l/t]

Greek

β . . . . ratio of probe to pipe diameter [unitless]
θ . . . . circumferential angle [radians]
ρ . . . . density [m/l^3]

References

Amir, I. and A. Peranio (1972) "Flow Measuring Device," U. S. Patent No. 3,768,754.

CTI (1995) "Standard for Water Flow Measurement," Bulletin STD-146, Cooling Technology Institute.

CTI (2000) "Acceptance Test Code for Water Cooling Towers," Code ATC-105, Cooling Technology Institute.

Gibson, G. H. (1918) "Simplex Pitot Tube," The Geo. H. Gibson Co., pp. 11-12, cited by Amir and Peranio, 1972.

Johnson, C. B. and D. M. Bushnell (1970) "Power-Law Velocity-Profile-Exponent Variations with Reynolds Number, Wall Cooling, and Mach Number, in a Turbulent Boundary Layer," NASA Technical Note D-5753.

Rudman, M., H. M. Blackburn, L. J. Graham, and L. Pullum (2001) "Weakly Turbulent Pipe Flow of a Power Law Fluid," Proceedings of the 14th Australasian Fluid Mechanics Conference, Adelaide, Australia.

Zanoun, E.-S., F. Durst, and H. Nagib (2003) "Evaluating the Law of the Wall in Two-Dimension Fully Developed Turbulent Channel Flows," ***Physics of Fluids***, Vol. 15, No. 10.